Local-density–functional approach to all-*trans*-polyacetylene

J. W. Mintmire and C. T. White
Code 6139, Naval Research Laboratory, Washington, D.C. 20375
(Received 7 April 1983)

A new first-principles self-consistent computational approach for determining the electronic properties of polymers is presented. The local-density–functional formalism in conjunction with a linear combination of atomic orbitals approximation is used to determine the geometry (by minimizing the total energy within a variational scheme) and electronic structure of periodic chain polymers. This method is applied to all-*trans*-polyacetylene, and leads to a theoretically calculated geometry, x-ray and ultraviolet photoelectron spectra, and dielectric function $\epsilon(q,\omega)$ in good agreement with experimentally determined values.

INTRODUCTION

Although the properties of wideband, quasi-one-dimensional polymers have long been a subject of interest,[1] a renewed concern[2] (both fundamental and applied) in such systems has occurred recently. Much of this work has been stimulated by the growth of films of polyacetylene,[3] polypyrrole,[4] and polyparaphenylene[5] that can be chemically doped to give large changes in their conductivity. Polyacetylene represents the simplest member of this family of electroactive polymers, and an extensive number of quantum-chemical (both *ab initio* and semiempirical) studies of this material have been undertaken.[6–15] The previous work demonstrates that large-scale Hartree-Fock (HF) calculations predict a reasonable equilibrium geometry for polyacetylene. However, the HF-based approaches have not produced a satisfactory electronic structure for polyacetylene. Typically, when compared to experimental data, the HF methods greatly overestimate the band gap at the Fermi level and also predict much too large a separation between the highest and lowest occupied valence bands. By analogy, similar problems are expected for related electroactive polymers. In contrast, the methods that predict a better overall one-electron spectrum[12] typically require knowledge of the geometry of the system. This requirement is unfortunate; due to difficulties in preparing single crystals, the details of the intrachain geometry often are not well known in quasi-one-dimensional polymers. For example, although the amount of dimerization at equilibrium geometry u_0 for *trans*-polyacetylene is crucial in understanding the system, this quantity only recently has been suggested experimentally.[16] The questions of geometry and the electronic structure in the vicinity of the Fermi level are linked in any Peierls distorted system.

In this paper we outline a new first-principles method for determining both the electronic structure and total energy of chain polymers, where the system of interest is considered an ensemble of essentially noninteracting periodic chains. We have used this method to calculate the total energy as a function of geometry, and the band structure of *trans*-polyacetylene. A preliminary description[17] of our energy minimization results for *trans*-polyacetylene has been given. In addition, we now report and compare experimental x-ray-photoelectron spectroscopy (XPS) and ultraviolet-photoelectron spectroscopy (UPS) results to spectra theoretically calculated from our electronic structure using first-principles photoelectron cross sections. We find that our theoretically predicted XPS and UPS spectra are in excellent agreement with experimental results. Also, we present theoretical results[18] for the anisotropic dielectric function $\epsilon(q,\omega)$ of *trans*-polyacetylene and discuss these results in comparison with experimental electron-energy-loss spectra[19] and optical spectra.[20,21] Our results for $\epsilon(q,\omega)$ agree with the experimentally observed plasmon dispersion relation observed by Ritsko *et al.*[19] These results also indicate that the electron energy loss observed at ~ 9 eV is due to polarizations perpendicular to the chain direction that result in π-σ^* excitations.

APPROACH

Our approach is based on a linear combination of atomic orbitals (LCAO) local-density–functional ($X\alpha$) scheme.[22] This formalism is related to that introduced by Mintmire *et al.*[23] for two-dimensionally periodic systems. The $X\alpha$ total-energy functional (in Hartree atomic units) is given by

$$\langle E\rangle = -\tfrac{1}{2}\sum_{i,k} n_i(k)\int_\Omega d^3r\,\phi_i^*(\vec{r};k)\nabla^2\phi_i(\vec{r};k) + U_C - U_X\ , \tag{1}$$

where Ω indicates integration over the appropriate unit cell and $n_i(k)$ is the occupation number of the one-electron wave function ϕ_i in the ith band with wave vector k. The total-energy functional is variationally minimized to yield the usual secular equation that is solved self-consistently to convergence. The one-electron wave functions $\phi_i(\vec{r};k)$ are linear combinations of Bloch functions $\chi_j(\vec{r};k)$ such that

$$\phi_i(\vec{r};k) = \sum_j c_{ji}(k)\chi_j(\vec{r};k)\ , \tag{2}$$

where the Bloch functions are sums of atom-centered s- and p-type Gaussian functions $U_j(\vec{r})$,

$$\chi_j(\vec{r};k)=\sum_m \exp[imak]U_j(\vec{r}-ma\hat{z}) , \quad (3)$$

and where the variable a is the unit-cell spacing. The Coulomb energy U_C is defined by

$$U_C=\tfrac{1}{2}[\rho-\rho_N \mid \rho-\rho_N] , \quad (4)$$

where

$$[\rho_a \mid \rho_b]=\int_\Omega d^3r_1 \int d^3r_2 \rho_a(\vec{r}_1)\rho_b(\vec{r}_2)/r_{12} , \quad (5)$$

and the interaction of a nuclear point charge with itself is taken to be zero. The charge density ρ is defined as

$$\rho(\vec{r})=\sum_{i,k} n_i(k) \mid \phi_i(\vec{r};k) \mid ^2 , \quad (6)$$

and ρ_N denotes the lattice of nuclear charges. The exchange energy U_X is defined (for non-spin-polarized systems) by

$$U_X=9\alpha(3/32\pi)^{1/3}\int_\Omega d^3r \rho^{4/3}(\vec{r}) . \quad (7)$$

The value of the exchange parameter α was set equal to the canonical value of $\frac{2}{3}$ for all calculations.

The one-electron effective Hamiltonian matrix elements are calculated in each iteration of the self-consistent procedure for the Bloch orbital basis set. These matrix elements were evaluated using fitting techniques related to those developed by Dunlap *et al.*[24] for molecular LCAO $X\alpha$ calculations. We have used the same formalism for fitting the Coulomb potential and exchange potential for polymers as was derived earlier for two-dimensionally periodic systems. Full details of this formalism may be found in Ref. 23; note that a frozen-core approximation is not used in our calculations. Owing to the long-range nature of the Coulomb interaction, computational difficulties typically are encountered in properly truncating lattice sums involving Coulomb terms. These problems have been handled by treating the electron and nuclear charges concomitantly in the fitting procedure. We also have incorporated in our approach multipole-expansion techniques based on the work of Piela and Delhalle[25] so that the Coulomb integrals contain all long-range multipole-interaction contributions up to octopole-octopole interactions. These techniques are important in decreasing the amount of computer time necessary for evaluating the Coulomb matrix elements as well as introducing long-range multipole-interaction effects in the band energies.

POLYACETYLENE ELECTRONIC STRUCTURE AND GEOMETRY

Because polyacetylene is a prototype system of considerable interest and much is known about this system, we chose *trans*-polyacetylene for initial study. Experimental evidence indicates that *trans*-polyacetylene is dimerized[16] at its equilibrium geometry with a π-π^* band gap of 1.4—1.8 eV (Refs. 26 and 27) and an estimated band gap for isolated chains of 1.8 eV.[28] In implementing our polyacetylene studies we used a $7s\,3p/3s$ basis set[29] and ten evenly spaced wave vectors to describe the one-dimensional Brillouin zone. As a preliminary to this choice of basis set, we made calculations on the ethylene molecule using the molecular LCAO $X\alpha$ method,[24] which is closely related to our approach. For the $7s\,3p/3s$ basis set these molecular calculations yielded an equilibrium C—C bond distance of 1.35 Å that compares favorably with the experimentally determined[30] bond distance of 1.34 Å. For simplicity in these molecular calculations and in our polyacetylene studies, all bond angles were constrained to equal 120° and all the C—H bond distances were fixed at the generally accepted value[11] of 1.08 Å.

We have determined the total energy per unit cell of the polyacetylene chain at eleven different geometries specified in Table I. Atomic total energies for carbon and hydrogen were calculated for the same $7s\,3p/3s$ basis set using the molecular LCAO $X\alpha$ method.[24] These calculations indicate a dimerized ground state for *trans*-polyacetylene with an equilibrium unit-cell length of 2.435 Å. The ground state is stabilized by 0.016 eV per CH unit relative to the lowest-energy undimerized state. This condensation-energy difference should not be confused with the thermal energy kT_P required to induce a Peierls transition; kT_P will be on the order of half the band gap E_g.[17,31] The calculated unit-cell length is in good agreement with the experimental value[16] of 2.46 Å and we expect this agreement to improve slightly if we relax the constraint of fixing all bond angles to a value of 120°. We obtain values of 1.377 and 1.434 Å for the short and long C—C bond distances occurring in the dimerized configuration. We do not expect the value of the unit-cell length to change more than a few percent in any larger basis-set calculation. However, we are not as confident of the accuracy of our predicted value of the equilibrium dimerization coordinate $u_0 \sim 0.02$ Å [as defined by Su, Schrieffer, and Heeger[32] (SSH)]. We have found that the energy difference between our ground-state dimerized geometry and some appreciably more dimerized configurations, up to $u \sim 0.03$ Å, is on the order of 25% of the E_{stab} value of 0.016 eV/CH unit. In view of this result, we think that the present $7s\,3p/3s$ basis set may provide

TABLE I. Calculated total energies per unit cell for all-*trans*-polyacetylene. The values r_1 and r_2 denote short and long carbon—carbon bond lengths, respectively. Binding energy is the total energy per unit cell minus the sum of atomic energies of two carbon atoms and two hydrogen atoms. Atomic energies for carbon and hydrogen are −37.073 827 and −0.452 765 hartrees, respectively.

r_1 (Å)	r_2 (Å)	Energy (hartrees)	Binding energy (eV)
1.35	1.45	−75.734 186	−18.530
1.35	1.48	−75.733 267	−18.505
1.36	1.43	−75.734 628	−18.542
1.36	1.45	−75.734 561	−18.540
1.36	1.48	−75.733 565	−18.513
1.38	1.45	−75.734 747	−18.545
1.38	1.48	−75.733 636	−18.515
1.377	1.434	−75.734 907	−18.550
1.36	1.36	−75.729 754	−18.409
1.40	1.40	−75.733 614	−18.515
1.44	1.44	−75.731 863	−18.467

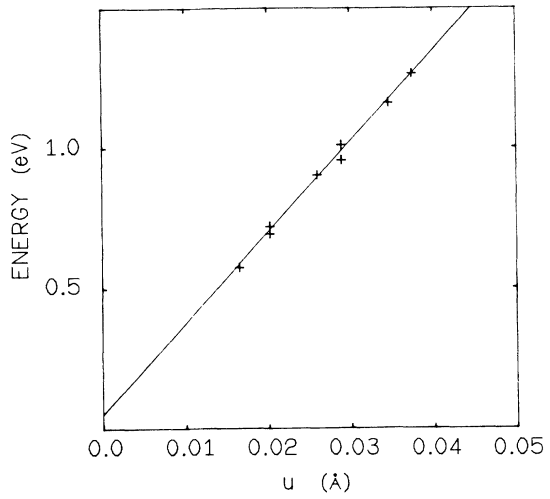

FIG. 1. Calculated band gap E_g vs dimerization coordinate u.

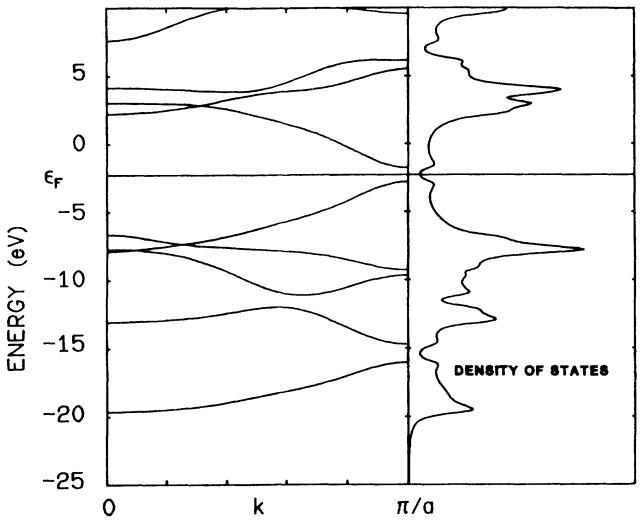

FIG. 2. Band structure and DOS resulting from this band structure for *trans*-polyacetylene. Energy ϵ_F denotes the Fermi level.

only a partially converged answer to the value of u_0 implied by Eq. (1). This result also shows that pursuing this question any further within the context of a single-chain calculation may not be profitable. Owing to these small energy differences, interchain interactions, for example, might play a prominent role in any final determination of u_0. However, extrapolating a comparison between the present results and those obtained using a smaller basis set ($4s\,2p/3s$) indicates that u_0 will probably increase with a larger basis-set calculation due to an improved description of the bonding. In addition, the results of the $4s\,2p/3s$ and $7s\,3p/3s$ calculations show that the total energy increases rather rapidly for values of u a little greater than 0.03 Å. These trends give us confidence that our present results restrict the actual value of u_0 implied by Eq. (1) to a value in the vicinity of $\sim 0.02 - \sim 0.03$ Å due to intrachain effects. This range of values for u_0 overlaps well with the experimentally suggested range[16] $0.02 \lesssim u_0 \lesssim 0.04$ Å.

We calculate that the one-electron band gap E_g at the Fermi level for our equilibrium geometry is 0.6 eV as compared to an experimentally suggested range of 1.4—1.8 eV. However, we can partially account for underestimating the experimental energy gap at the Fermi level if the u_0 of the actual polymer is somewhat larger than we predict. For example, we have shown that the present method yields an E_g of 1 eV if we assume that $u_0 = 0.03$ Å. Because the $X\alpha$ method typically underestimates gaps by 30—50% when compared to experimental data,[33] we would not expect the agreement between our predicted E_g and experimental values to improve appreciably with further $X\alpha$ calculations. Indeed, this analysis suggests that u_0 for the polymer is probably closer to 0.03 than 0.02 Å. Thus, in the following sections we will use band-structure results corresponding to our predicted unit-cell length and $u_0 = 0.03$ Å in our calculations of the electronic properties of *trans*-polyacetylene. As depicted in Fig. 1, we have shown to an excellent approximation that our predicted E_g obeys the linear relationship $E_g = \gamma u$, with $\gamma = 32.4$ eV/Å, and where u denotes the amount of dimerization. Also, these band-structure results are consistent with those previously reported by Grant and Batra[12] using non-self-consistent local-density—functional methods.

The band-structure and effective one-electron density of states (DOS) for the valence bands and the first few conduction bands, calculated by assuming our predicted unit-cell length and $u_0 = 0.03$ Å, are presented in Fig. 2. We have found that the band structure is rather insensitive to the dimerization except at the zone boundary where gaps appear. On the other hand, we have found that the band structure is sensitive to the unit-cell length. The DOS shown in Fig. 2 has been smoothed by convoluting our results with a 0.6-eV-wide Lorentzian. To calculate the photoelectron spectra we use the first-order time-dependent perturbation-theory result given by Smith,[34]

$$d\sigma_i(\vec{k}_f) = \frac{e^2 L^3 k_f}{6\pi mc\omega} \left| \int_\Omega d^3r\, u^*_{\vec{k}_f}(\vec{r}) \vec{\nabla} u_i(\vec{r}) \right|^2 d\hat{k}_f \,, \tag{8}$$

where u_i is the initial state obtained from our self-consistent calculations and $u_{\vec{k}_f}$ is the final state. For the purposes of this analysis $u_{\vec{k}_f}$ is assumed to be well described using a plane wave with propagation vector $\vec{k}_f$ which satisfies energy conservation. We have spherically averaged the photoelectron cross section in Eq. (8) to describe experimental results that typically do not angularly resolve the cross sections. Line-shape results for incident-photon energies of 40.8 and 1254 eV, corresponding to UPS and XPS photon energies, respectively, are depicted in Fig. 3. These results are compared with the raw experimental XPS spectrum of Brundle reported by Grant and Batra[12] and the raw UPS spectrum of Salaneck *et al.*[35] The absorption edge of the XPS spectrum has been shifted to match the theoretical threshold and the

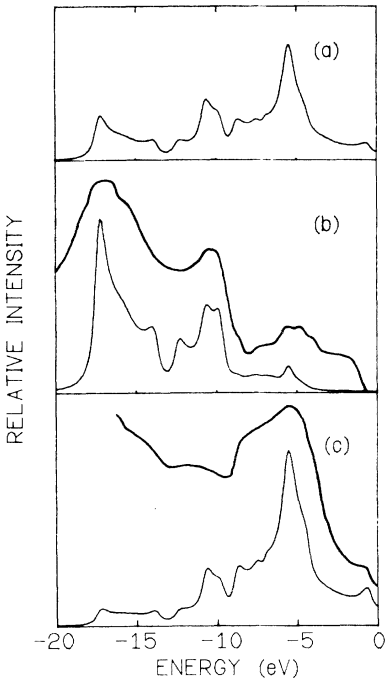

FIG. 3. (a) DOS for all-*trans*-polyacetylene, (b) theoretical and experimental XPS spectra for *trans*-polyacetylene, and (c) theoretical and experimental UPS spectra for *trans*-polyacetylene. Upper lines in (b) and (c) represent experimental results and lower lines represent theoretical results. No background subtraction has been made for the experimental results.

UPS data have been aligned by assuming a work function of 4.5 eV. If a straight-line background subtraction of the experimental data is assumed, excellent agreement between the theoretical and experimental line shapes is found for both the XPS and UPS spectra. We believe these are the first reported results obtained by using first-principles methods to reasonably predict the location of the -17-eV XPS peak.

Finally, we were interested to see to what extent our results for the π band are consistent with some of the assumptions made about this band in the SSH model.[32] The SSH model supposes that this π band can be described by a Hamiltonian of the form

$$H=\sum_i |i\rangle\epsilon_0\langle i| +\sum_{i,j} |j\rangle V_{ij}\langle j| \ , \tag{9}$$

where ϵ_0 is assumed independent of u, and $V_{ij}=V_0+2\alpha u$ if i,j indicate nearest neighbors; otherwise $V=0$. A Hamiltonian of this form predicts that the Fermi level, as well as the bottom of the π band, is independent of u and that the width of the occupied portion of the π band depends only on the long bond distance. To a good approximation, we find all three of these assumptions are satisfied over the range of dimerizations of interest. The value of V_0 that we obtain from this analysis is -2.75 eV, in good agreement with values that have been assumed[32] for this parameter. Within the SSH model, E_g is given by $E_g=8\alpha u$. As mentioned, we find that our calculated E_g obeys a relationship of the form $E_g=\gamma u$, and therefore our predicted value of the electron-phonon–coupling constant α from the π band is 4.1 eV/Å. The value of α is smaller than the most recently suggested empirical value of this parameter (7.1 eV/Å). However, given the $X\alpha$ model's tendency to underestimate gaps, this difference is to be expected. Indeed, if we suppose that the actual gap is between 1.4 and 1.8 eV and is related to the $X\alpha$ gap by the relation $E_g=\beta E_g^{X\alpha}$, with β independent of u, then our previous result for $E_g^{X\alpha}$ at the experimentally suggested dimerization value implies that β lies between 1.4 and 1.8. This analysis then leads to a predicted value of α between 5.7 and 7.4 eV/Å.

DIELECTRIC RESPONSE PROPERTIES

Several recent experimental studies using techniques such as electron-energy-loss spectroscopy[19] (EELS) and synchrotron-radiation-reflectivity measurements[20] have yielded extensive information on the electronic response properties of *trans*-polyacetylene. These properties are described theoretically by the dielectric function $\epsilon(q,\omega)$. In a preliminary report of this work[18] we presented a theoretical first-principles description of the longitudinal dielectric function for polarizations parallel to the polyacetylene-chain axis. The anisotropy of this system requires, however, that a full treatment of the dielectric function include the response to polarizations perpendicular to the chain axis. We have examined these anisotropic effects, in addition to the dielectric response due to polarizations parallel to the chain axis, and describe our results below.

In our calculation we use the self-consistent longitudinal dielectric constant $\epsilon(q,\omega)$ derived by Ehrenreich and Cohen,[36]

$$\epsilon(q,\omega)=1+\frac{4\pi e^2}{q^2\Omega}\sum_{m,m',k}\frac{|(m,k\,|\,m',k+q)|^2}{\hbar\omega+E_{m',k+q}-E_{m,k}} \times[f_0(E_{m',k+q})-f_0(E_{m,k})] \ , \tag{10}$$

where Ω is the volume per C_2H_2 unit and all notation is as that used by Adler.[37] The sums over m and m' refer to sums over both filled and empty bands. To evaluate Eq. (10) at $q=0$, we use the identity[37]

$$(m,k\,|\,m',k+q)=\frac{\hbar q(m,k\,|\,\{p+\hbar k+\hbar q\}\,|\,m',k+q)}{\{m(E_{m',k+q}-E_{m,k})\}} \tag{11}$$

for the case of all vectors along the chain axis.

For the one-electron wave functions $|m,k)$ and band energies used in Eq. (10), we calculate the longitudinal response for polarizations parallel to the chain axis in an ideal one-dimensionally periodic chain of polyacetylene using the same LCAO $X\alpha$ self-consistent, one-dimensional band-structure results used to obtain Fig. 2. Our calculations do not include interchain or disorder effects within the crystalline geometry reported by Fincher *et al.*[16] In

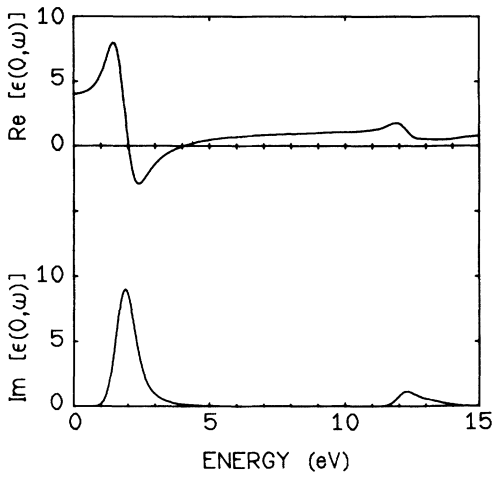

FIG. 4. Calculated optical dielectric function $\epsilon(0,\omega)$ vs energy for all-*trans*-polyacetylene.

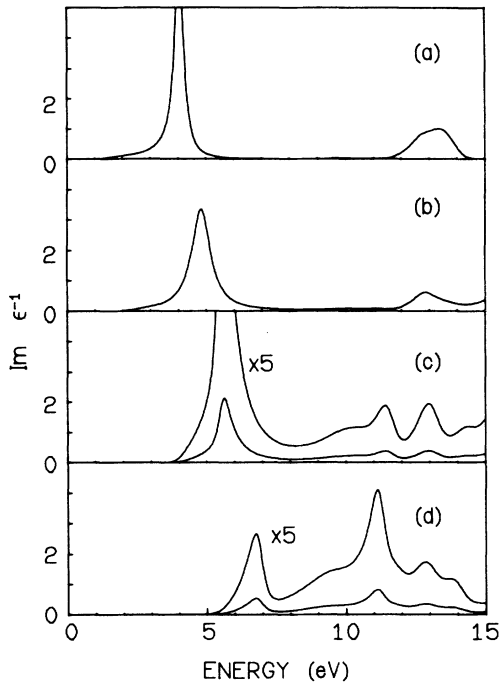

FIG. 5. Predicted electron-energy-loss spectra as a function of electron momentum q for the following values of q: (a) 0, (b) 0.26, (c) 0.52, and (d) 0.78 Å^{-1}.

evaluating Eq. (10) all occupied bands have been shifted down by 0.8 eV to yield a one-dimensional band gap in agreement with experiment of 1.8 eV.[28] This level shift corrects the previously mentioned well-known tendency of local-density–functional models to underestimate the band gaps[33] and is an ansatz which simulates the effect of introducing a self-interaction correction[38] in an appropriate manner for the purposes of this analysis. For the volume per C_2H_2 unit (Ω) in Eq. (10), we use the value corresponding to the measured bulk density[26] of 0.4 g/cm^3. Using this value corresponds to calculating the macroscopic response of the system and incorporates the effects of voids between polyacetylene fibrils. Because we are interested in energies for $\epsilon(q,\omega)$ under 15 eV, we consider only the π and π^* bands at the Fermi level as well as the two highest occupied and two lowest unoccupied σ bands. These bands describe all interband excitations less than 15 eV which cross the Fermi level. As a result of our numerical methods, the imaginary part ϵ_2 of the calculated $\epsilon(q,\omega)$ has been broadened by a Gaussian smoothing function of half-width 0.35 eV to damp oscillations arising from the numerical algorithms used. Calculations using less broadening indicated that the major features of our results [$\epsilon(0,0)$ and the plasmon dispersion relation] are relatively insensitive to this amount of broadening. The real part ϵ_1 of the dielectric function was calculated from $\epsilon_2(q,\omega)$ using a Kramers-Kronig analysis.

We calculated $\epsilon(q,\omega)$ for polarizations parallel to the chain axis ($\epsilon_{||}$) over a range of ω between 0 and 15 eV and for the discrete set of q values (where q is the magnitude of the momentum-transfer vector parallel to the chain axis) of 0.0, 0.26, 0.52, and 0.78 Å^{-1}. Our results for $\epsilon_{||}(0,\omega)$ are depicted in Fig. 4. The calculated value of 4.0 for the dielectric constant $\epsilon(0,0)$ agrees well with experimental results obtained from optical-absorption data[26] on oriented *trans*-polyacetylene having a density equal to the density we used in our calculations. The shape of $\epsilon(0,\omega)$ in Fig. 4 for energies less than 4 eV is consistent with those from previous experimental data[26] and earlier tight-binding approaches.[32]

Figure 5 presents our calculated results for the energy-loss spectra of polyacetylene obtained from $\epsilon_{||}$ at these values of q. As can be seen from Fig. 4, the peak in $\text{Im}[1/\epsilon(0,\omega)]$ at 4.0 eV [Fig. 5(a)] can be interpreted as a plasmon because ϵ_1 is zero and ϵ_2 is small and decreasing in this region. This is also true of the peaks in Figs. 5(b) and 5(c), where q is equal to 0.26 and 0.52 Å^{-1}, respectively, but not so for $q=0.78$ Å^{-1} in Fig. 5(d). Our results imply that ϵ_1 for this value of q (not shown) is positive for all energies under 15 eV. A comparison of our calculated plasmon positions with those of the experimental energy-loss spectra[1] is depicted in Fig. 6. Except for $q=0.78$ Å^{-1}, this figure illustrates the excellent agreement between our predicted linear relationship for the plasmon peaks and experimental results. Because our results are dependent on the volume per CH unit, the exact amount of agreement with experiment, as indicated in Fig. 6, is somewhat fortuitous. However, for values of Ω within 20% of the above-mentioned value, good agreement is maintained with experimental data.[39] Our results indicate that the linear plasmon dispersion is primarily due to the π and π^* bands being basically parallel in the region of the energy gap, which is the region having most effect on ϵ_2. By being parallel we mean in the sense of being collinear across the Brillouin-zone edge at π/a in an unfolded Brillouin scheme. This is consistent with the previous interpretation of this mechanism based on a tight-binding analysis.[19]

Our calculated results indicate only two major peaks in $\text{Im}\epsilon_{||}$. At $q=0$ these peaks correspond to a π-π^* transi-

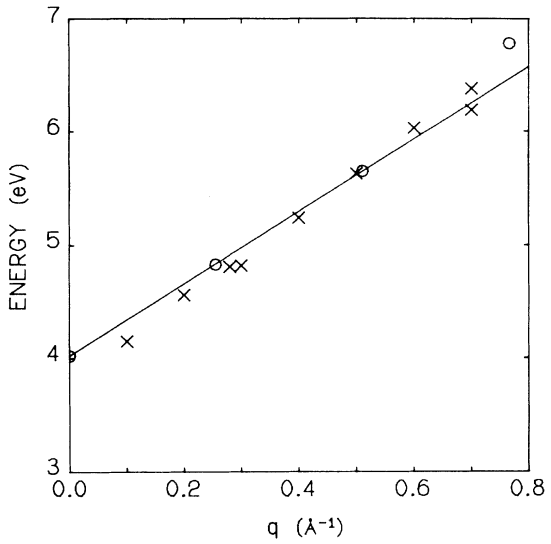

FIG. 6. Calculated and experimental plasmon peaks from electron-energy-loss spectra vs electron momentum. Cross marks (×) indicate the experimental results of Ritsko *et al.* (Ref. 19) and open circles (○) indicate our calculated plasmon-peak locations as a function of q.

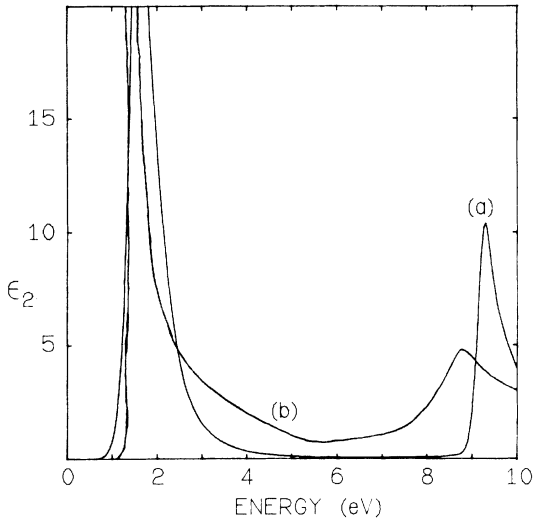

FIG. 7. (a) Imaginary component of theoretically calculated average dielectric function $\tilde{\epsilon}(0,\omega)$, and (b) imaginary component of experimentally derived average dielectric function ϵ observed by Ritsko *et al.* Note experimental results are for the minimum reported momentum transfer of 0.1 Å^{-1}.

tion at about 2 eV and a transition between σ bands at about 12 eV. Ritsko[19] reports an essentially dispersionless peak at about 9 eV and a peak at about 2.4 eV with small dispersion, which is apparently hidden by the π-π^* transition at small q. We believe that the 2.4-eV peak results from three possible causes. The first possibility is an excitonic enhancement of the absorption edge as described by Ritsko.[19] This process will not be described within an interband-transition model, such as we are using, although our results are consistent with this process. The second process is a broadening of ϵ_2 due to lack of orientation of the crystallites. This causes ϵ_2 to be a spatial average over all orientations of q where the effective value of q is given by the component of q parallel to the chain axis. Ritsko[19] indicates this as a possible mechanism but points out that this mechanism would require very strong matrix-element effects to describe the experimental data. Our results, however, indicate the matrix elements for excitations across the fundamental gap are indeed large and may well be another source of the 2.4-eV peak in addition to excitonic enhancement. The third possibility arises from the strong electron-phonon coupling expected in *trans*-polyacetylene. This coupling should result in a general broadening of any electronic transitions. The phonon-assisted transition discussed in our preliminary report[18] would result in a general broadening of $\mathrm{Im}[\epsilon(q,\omega)]$ toward that expected from the joint DOS.

From Eq. (10) we have calculated the dielectric response at $q=0$ for polarizations perpendicular to the polyacetylene-chain axis $\epsilon_\perp(0,\omega)$. These results indicate a large dielectric response (i.e., $\mathrm{Im}\epsilon_\perp$ is large) at about 9 eV for the polarizations perpendicular to the plane formed by the carbon backbone. This response arises from the interband transitions between the occupied π band and the lowest unoccupied σ^* band. From a tight-binding analysis one can observe that these transitions include nonzero single-site matrix elements (as opposed to nearest-neighbor matrix elements being the leading nonzero contribution for σ-σ^* and π-π^* transitions) in Eq. (10). As a result, these transition matrix elements are reasonably large. This factor, as well as the π and σ^* bands being effectively parallel for a large portion of the Brillouin zone near the band edge, leads to a large contribution to the dielectric function near 9 eV by polarizations capable of exciting this transition.

The experimental results reported by Ritsko *et al.*[19] and displayed in Fig. 6 represent an average response of the system. These results for $\mathrm{Im}[\epsilon(q,\omega)]$ were obtained from a Kramers-Kronig analysis of the energy-loss spectra which are proportional to $\mathrm{Im}[1/\epsilon(q,\omega)]$. Ritsko evaluated the absolute magnitude of the experimentally derived ϵ by requiring the dielectric constant $\epsilon(0,0)$ have a value of 10. To compare our theoretical results with these experimental results we calculated an average dielectric function $\tilde{\epsilon}(0,\omega)$ constructed according to the following method. First, we calculated the theoretical energy-loss spectra ($\mathrm{Im}[1/\epsilon]$) for polarizations both parallel and perpendicular to the chain axis. Next, we constructed an average predicted energy-loss spectrum $\langle \mathrm{Im}[1/\epsilon] \rangle$ from the spherical average of the theoretical $\mathrm{Im}[1/\epsilon]$ over all possible polarization orientations. Last, we calculated an average dielectric function $\tilde{\epsilon}$ [defined by $1/\tilde{\epsilon}=\langle \mathrm{Re}[1/\epsilon] \rangle + i\langle \mathrm{Im}[1/\epsilon] \rangle$] by using the same Kramers-Kronig analysis used for interpreting the experimental results by Ritsko *et al.* This average dielectric response is shown in Fig. 7.

From these results we interpret the observed experimental peak at 8–9 eV as due to polarizations perpendicular to the chain backbone. Although our current calculations for polarizations perpendicular to the chain axis were only

performed for $q=0$, the response due to these polarizations should be relatively dispersionless due to small interchain-interaction matrix elements. This prediction is in agreement with the experimentally observed lack of dispersion in the EELS-derived $\epsilon(q,\omega)$ peak at 8–9 eV and our results provide a new interpretation of this peak.

SUMMARY AND CONCLUDING REMARKS

We have outlined a new self-consistent LCAO $X\alpha$ approach for predicting the properties of periodic-chain polymers. Our work demonstrates for the first time the utility of a LCAO $X\alpha$ approach in obtaining the ground-state geometries, XPS, UPS, and dielectric response of these polymers. When compared to experimental data the results we have reported for *trans*-polyacetylene provide substantial evidence that the methods described can be used informatively to study a wide range of properties of other electroactive polymers. These methods are not restricted to such polymers but can be used to study, for example, piezoelectric polymers of current interest as well as various insulating covalent chain polymers such as polyethylene. When coupled with pseudopotential techniques, our approach should also be useful in studying higher-dimensional systems.

ACKNOWLEDGMENTS

We would like to thank D. L. Peebles and M. L. Elert for many helpful discussions. One of us (J.W.M.) acknowledges the support of the National Research Council through the National Research Council–Naval Research Laboratory (NRC-NRL) Cooperative Postdoctoral Associateship program. This work was supported in part by U. S. Navy Office of Naval Research Contract No. N0001481WR10010.

[1]See, e.g., J. E. Lennard-Jones, Proc. R. Soc. London Ser. A 158, 280 (1937); C. A. Coulson, *ibid.* 169, 413 (1939); H. C. Longuet-Higgins and L. Salem, *ibid.* 251, 172 (1959).

[2]See, e.g., papers and references therein in Synth. Met. 1 (1979/1980); Mol. Cryst. Liquid Cryst. 77 (1981).

[3]H. Shirakawa, E. J. Louis, A. G. MacDiarmid, C. K. Chiang, and A. J. Heeger, J. Chem. Soc. Chem. Commun. 578 (1977).

[4]K. K. Kanazawa, A. F. Diaz, R. H. Geiss, W. D. Gill, J. F. Kwak, J. A. Logan, J. F. Rabolt, and G. B. Street, J. Chem. Soc. Chem. Commun. 854 (1979).

[5]D. M. Ivory, G. G. Miller, J. M. Sowa, L. W. Shacklette, R. R. Chance, and R. H. Baughman, J. Chem. Phys. 71, 1506 (1979).

[6]J. M. Andre and G. Leroy, Int. J. Quantum Chem. 5, 557 (1971); J. M. Andre, G. S. Kapsomenos, and G. Leroy, Chem. Phys. Lett. 8, 195 (1971).

[7]J. E. Falk and R. J. Fleming, J. Phys. C 8, 627 (1975).

[8]M. Kertesz, J. Koller, and A. Azman, J. Chem. Phys. 67, 1180 (1977); J. Chem. Soc. Chem. Commun., 575 (1978).

[9]C. B. Duke, A. Paton, W. R. Salaneck, H. R. Thomas, E. W. Plummer, A. J. Heeger, and A. G. MacDiarmid, Chem. Phys. Lett. 59, 146 (1978).

[10]V. Young, S. H. Suck, and E. W. Hellmuth, J. Appl. Phys. 50, 6088 (1979).

[11]A. Karpfen and J. Pekov, Solid State Commun. 29, 251 (1979); Theor. Chim. Acta (Berlin) 53, 65 (1979).

[12]P. M. Grant and I. P. Batra, Solid State Commun. 29, 225 (1979); Synth. Met. 1, 193 (1979/80).

[13]R. V. Kasowski, E. Caruthers, and W. Y. Hsu, Phys. Rev. Lett. 44, 676 (1980); R. V. Kasowski, W. Y. Hsu, and E. Caruthers, J. Chem. Phys. 72, 4896 (1980).

[14]S. Suhai, J. Chem. Phys. 73, 3843 (1980).

[15]J. L. Bredas, R. R. Chance, R. Silbey, G. Nicolas, and Ph. Durand, J. Chem. Phys. 75, 255 (1981).

[16]C. R. Fincher, C.-E. Chen, A. J. Heeger, and A. G. MacDiarmid, Phys. Rev. Lett. 48, 100 (1982).

[17]J. W. Mintmire and C. T. White, Phys. Rev. Lett. 50, 101 (1983).

[18]J. W. Mintmire and C. T. White, Phys. Rev. B 27, 1447 (1983).

[19]J. J. Ritsko, Phys. Rev. B 26, 2192 (1982); J. J. Ritsko, E. J. Mele, A. J. Heeger, A. G. MacDiarmid, and M. Ozaki, Phys. Rev. Lett. 44, 1351 (1982).

[20]T. Mitani, S. Suga, Y. Tokura, K. Koyama, I. Nakada, and T. Koda, Int. J. Quantum Chem. 18, 655 (1980); T. Mitani (private communication).

[21]D. Baeriswyl, G. Harbeke, H. Kiess, E. Meier, and W. Meyer (unpublished).

[22]For a review of the $X\alpha$ method, see J. W. D. Connolly in *Modern Theoretical Chemistry*, edited by G. A. Segal (Plenum, New York, 1976), Vol. 7, and references therein.

[23]J. W. Mintmire, J. R. Sabin, and S. B. Trickey, Phys. Rev. B 26, 1743 (1982).

[24]B. I. Dunlap, J. W. D. Connolly, and J. R. Sabin, J. Chem. Phys. 71, 3396 (1979).

[25]L. Piela and J. Delhalle, Int. J. Quantum Chem. 13, 606 (1978).

[26]C. R. Fincher, M. Ozaki, M. Tanaka, D. Peebles, L. Lauchlan, A. J. Heeger, and A. G. MacDiarmid, Phys. Rev. B 20, 1589 (1979).

[27]T. Tani, P. M. Grant, W. D. Gill, G. B. Street, and T. C. Clarke, Solid State Commun. 33, 499 (1980).

[28]D. Moses, A. Feldblum, E. Ehrenfreund, A. J. Heeger, T.-C. Chung, and A. G. MacDiarmid, Phys. Rev. B 26, 3361 (1982).

[29]For Gaussian basis sets for the atoms H–Ne, see F. B. van Duijneveldt, IBM Report RJ 945 (1971) (unpublished).

[30]G. Herzberg, *Electronic Spectra and Electronic Structure of Polyatomic Molecules* (Van Nostrand and Reinhold, New York, 1966).

[31]See, for example, M. J. Rice and S. Strassler, Solid State Commun. 13, 125 (1973).

[32]W. P. Su, J. R. Schrieffer, and A. J. Heeger, Phys. Rev. Lett. 42, 1698 (1979); Phys. Rev. B 22, 2099 (1980).

[33]S. B. Trickey, A. K. Ray, and J. P. Worth, Phys. Status Solidi B 106, 613 (1981).

[34]K. Smith, *The Calculation of Atomic Collision Processes* (Wiley-Interscience, New York, 1971).

[35]W. R. Salaneck, H. R. Thomas, R. W. Bigelow, C. B. Duke, E. W. Plummer, A. J. Heeger, and A. G. MacDiarmid, J. Chem. Phys. 72, 3674 (1980); W. K. Ford, C. B. Duke, and A. Paton, J. Chem. Phys. 77, 4564 (1982); W. R. Salaneck (private

communication).
[36]H. Ehrenreich and M. H. Cohen, Phys. Rev. 115, 786 (1959).
[37]S. L. Adler, Phys. Rev. 126, 413 (1962).
[38]J. P. Perdew and A. Zunger, Phys. Rev. B 23, 5048 (1981), and references therein.
[39]Use of the crystallographic density of 1.1 g/cm^3 (Ref. 16) results in less plasmon dispersion with the largest differences occurring in the small-q results. The good agreement we obtain by assuming the bulk density of 0.4 g/cm^3 may result from screening from high-energy interband excitations not included in this calculation. In addition, for small q the wavelength corresponding to q and thus the plasmon wavelength will be of the order of the fibril diameter and thus void effects may need to be incorporated by assuming an effective medium with a density close to that of the bulk density.